

Passive Random Walkers and River-like Networks on Growing Surfaces

Chen-Shan Chin

Department of Physics, University of Washington,
P.O. Box 351560, Seattle, Washington 98195-1560

(Dated: May 21, 2019)

Abstract

Passive random walker dynamics is introduced on a growing surface. The walker is designed to drift upward or downward and then follow specific topological features, like hill tops or valley bottoms, of the fluctuating surface. The passive random walker can thus be used to directly explore scaling properties of such otherwise somewhat hidden topological features. For example the walker allows us to directly measure the dynamical exponent of the underlying growth dynamics. We use Kardar-Parisi-Zhang (KPZ) type surface growth as example. The world lines of a set of merging passive walkers show nontrivial coalescence behaviors and display the river-like network structures of surface ridges in space-time. In other dynamics, like Edward-Wilkinson growth, this does not happen. The passive random walkers in KPZ type surface growth is closely related to the shock waves in the noiseless Burgers equation. We also briefly discuss the relation with the passive scalar dynamics in turbulence.

I. INTRODUCTION

Fluctuations of surfaces during growth is one of the main subjects of nonequilibrium statistical mechanics in recent decades. Most research is focused on identifying the universality class and the scaling behavior of the surface morphology, e.g., how the surface width scales with the surface size [1, 2, 3, 4, 5, 6]. The coupling between surface growth and other degrees of freedom has also been considered recently in the context of ordering phenomena on growing and fluctuating surfaces. For example, the field coupled to the surface can be different species of deposited particles [5, 7, 8] or surface reconstruction order parameters [9]. Unlike in equilibrium surfaces, where the coupling between the surface height degrees of freedom and the additional field is irrelevant at large length scales [10], we found that the coupling between the surface and reconstruction order can not be ignored [9]. The surface and the additional field usually are coupled topologically. For example, the domain walls of order parameters become trapped at the hill tops or in the valleys of the surface for $1+1$ D system [5, 7, 8] or on the ridge lines of the surface for $2+1$ D system [9].

The fluctuations of the additional degrees of freedom (expressed by the dynamics of the "domain walls") thus become slaved to the fluctuations of the surface. From the surface perspective, the additional field is usually irrelevant and passive. Therefore, part of the dynamics of the surface and its topological features can be evaluated from the fluctuations of such domain walls that are pinned or trapped to them. We can put probes on the surface to follow these features dynamically. In this paper, the passive random walker (PRW) is designed to follow hill tops or valley bottoms of the surface.

One of the first application is to provide a direct way to measure the dynamical exponent of the surface fluctuations. We will also present the phenomena of coalescence of passive random walkers on Kardar-Parisi-Zhang (KPZ) [1, 2] type growth. The coalescence of passive random walkers uncovers a river-like network structure of the surface.

Our passive random walker is similar to passive scalars in turbulence. This is not surprising because the KPZ equation is equivalent to the Burgers equation describing a random stirred fluid [1] in which the random stirring force is different in nature from that in related turbulence studies. It is instructive to study the dynamics of the PRW from both perspectives.

This paper is organized as following. The passive walkers model is defined in Sec.II. The

application of directly measuring the dynamical exponent is presented in Sec. III. Then we discuss the coalescence of the PRW in Sec. IV. The sign of the coupling between the PRW and the surface is important for the coalescence phenomena as discussed in Sec. VI. In Sec. VII, we show the river-like network in the space-time structure of KPZ-type surfaces and the relation between the passive walker and the passive scalars in turbulence is briefly discussed. Other possible applications of the PRW model pointed out together with a summary of the results are in Sec. VIII.

II. PASSIVE RANDOM WALKER ON A GROWING SURFACE

We couple a PRW to the growth dynamics of a fluctuating surface. The movement of the PRW is determined by the local slope of the growing surface. The well-known Kin-Kosterlitz (KK) model [2] for surface growth is used as example. In the KK model, a surface is specified by integer height variables on a square lattice. A single particle is deposited at a randomly chosen site i if the restricted solid-on-solid condition ($|h_{ij} - h_j| \leq 1$ for all nearest neighbor pairs ij) remains satisfied, otherwise, the deposition of the particle is rejected. The surface grows and the stationary state is rough. The position of the PRW is updated after $N_s^2 = v_g M$ Monte Carlo steps (with v_g the growth velocity and N_s the total number of sites), i.e., when on average one layer of surface material is added, according to the following rules. Let i be the position of the walker. If there is any neighbor site j for which $h_j > h_i$, then we move the walker to site j . If there is more than one site higher than site i , then we let the PRW move to either one with equal probability. We apply periodic boundary conditions for both the surface and the PRW motion.

It is known that the continuum limit of the KK model is governed by the so called KPZ equation [2],

$$\frac{\partial h}{\partial t} = \frac{\partial^2 h}{\partial x^2} + \frac{\partial h}{\partial x} \xi + \eta \quad (1)$$

with uncorrelated noise,

$$h_s(\mathbf{x}; t) - h_s(\mathbf{x}^0; t^0) = D \int_{\mathbf{x}^0}^{\mathbf{x}} \int_{t^0}^t \xi(\mathbf{x}; \mathbf{x}^0) \quad (2)$$

In the same limit, the equation of motion of the PRW is

$$\frac{\partial u}{\partial t} = \frac{\partial}{\partial x} h(\mathbf{x}; t) \Big|_{\mathbf{x}=u(t)} \quad (3)$$

where $u(t)$ is the coordinate of the PRW at time t , and λ is the coupling strength between the PRW and the surface. In our lattice model, λ is of the same order as σ . The equations of motion, Eqs.(1)–(3), imply that the PRW moves upwards for $\lambda > 0$. The PRW becomes trapped on a local maximum of the surface profile as seen in Fig.(1) for positive λ . Once the PRW is trapped on a hilltop, the PRW follows the motion of the hilltop, and is subject to the surface fluctuations. When λ is negative, the PRW moves downwards instead of upwards, and the PRW becomes trapped in a valley bottom instead of a hilltop. We will focus on positive λ for now, and discuss negative λ in Sec.VI.

III. DYNAMICAL EXPONENT OF PASSIVE RANDOM WALKERS

One important observation of the dynamics of an upwards moving PRW on KPZ-type surfaces is that the PRW not only reaches a local maximum in a relatively short time but also that in finite size systems it ultimately ends up trapped at the global maximum. We will discuss the mechanism of this phenomena later in Sec.IV. Once the PRW is trapped on the global maximum, it performs a correlated random walk following the global surface fluctuations. The surface fluctuates critically and is self-affine. Namely, the profile of the surface is invariant under the following rescaling,

$$x \rightarrow b^{-1}x; h \rightarrow b^{-\alpha}h; t \rightarrow b^{-1+z_s}t; \quad (4)$$

where b is a scaling factor, α is the roughness exponent, and z_s is the dynamical exponent of the surface. The PRW is slaved to the fluctuations of the interface, therefore, we expect similar dynamical scaling for the world line of the PRW.

The displacement of the PRW, $u(t) = u(t) - u(0)$, should be defined carefully to avoid confusion in finite size systems with periodic boundary conditions, where the PRW moves on a ring in 1D and on a torus in 2D. In such manifolds, the winding number of the PRW should be taken into account. The component of the displacement, $u_{\hat{e}_i}(t)$, for direction \hat{e}_i is defined as $u_{\hat{e}_i}(t) = n_{\hat{e}_i}^+ - n_{\hat{e}_i}^-$, with the actual number of right moves, $n_{\hat{e}_i}^+$, and the actual number of left moves, $n_{\hat{e}_i}^-$ in direction \hat{e}_i .

In our numerical simulations, we let the system evolve until both the surface and the PRW motion reach the stationary state. Then the value of the displacement $u(t)$ is measured as

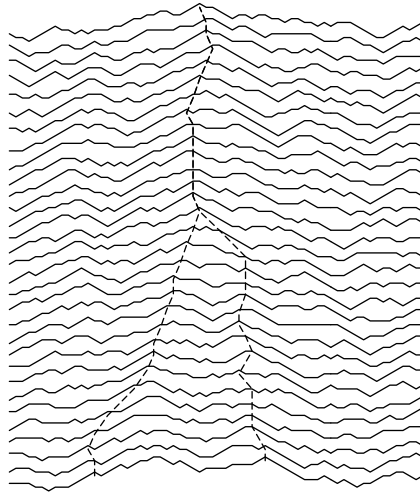


FIG . 1: Passive walkers trapped on local hill tops and global maximum in 1+ 1 D simulations. The dash lines are the world lines of two PRW s and the solid lines are the surface profiles during growth. The passive walkers follow the local maximum s initially and merge into each other ultimately. The walkers reach to the global maximum at a later time.

$u(t) = \sum_i^P n_{e_i}^+ n_{e_i}^{-2} t^{-1=2}$. To accelerate the simulation, we also adapt a rejection free algorithm. Detail of this algorithm can be found in ref.[9]. In this algorithm time is counted in terms of the numbers of layers of particles deposited instead of the conventional Monte Carlo time unit. We established earlier that the unit of time in this rejection free algorithm is linear proportional to the Monte Carlo time unit [9] (see also [8]).

If the PRW indeed is slaved to follow the global surface fluctuations, which are invariant statistically under the transformation eq.(4), the average distance of the displacement, $u(t)$, must obey the scaling form,

$$\langle u(t) \rangle \sim L G \left(\frac{t}{L^{z_s}} \right); \quad (5)$$

where $G(\cdot)$ is a universal scaling function. When $t \ll L^{z_s}$, the hopping events of the PRW are correlated due to the surface fluctuations, and $u(t) \sim t^{z_w}$, where z_w is the dynamical exponent for the PRW. At time scales $t \gg L^{z_s}$, the surface fluctuations are limited by the finite size of the lattice and the PRW becomes like a free uncorrelated random walker. Thus, the scaling function $G(\cdot)$ has the asymptotic forms, $G(\cdot) \sim t^{-1=z_w}$ for $t \ll 1$ and $G(\cdot) \sim t^{-1=2}$ for $t \gg 1$. The value of the exponent in Eq.(5) follows from the fact that $u(t)$ must be independent of L in the thermodynamic limit. Consequently, z_w and z_s are not independent and satisfy the relation $z_w = \frac{z_s}{2}$.

The dynamical exponent of the walker is not necessarily the same as the dynamical exponent of the surface. There is no priori reason for $z_w = 1$, i.e., for $z_w = z_s$. The numerical results (Fig. 2) indicate that $z_w = z_s$, but why? $z_w = 1$ reflects that there is no length scale other than the system size L involved in the dynamics of the PRW. This is in contrast to when the PRW performs free uncorrelated random walks, in which case another length scale proportional to $t^{-1=2}$ will emerge. The absence of an independent new length scale introduced is consistent with our picture that the PRW is typically trapped on a global maximum, hence the fluctuations of the PRW follow the dynamical scaling of the surface.

The main numerical results are shown in Fig.(2)-(4). They are obtained by averaging over about 10^5 samples in 1+1D and 4×10^5 samples in 2+1D. The displacements of the PRW are determined up to $t = 256$ in 1+1D and $t = 128$ in 2+1D. In 1+1D, $\langle u \rangle$ is in the order of 10^2 lattice units at $t = 256$. In 2+1D, $\langle u \rangle \sim 10$ at $t = 128$. Although $\langle u \rangle$ is relatively small in 2+1D, the scaling behaviors are already clear. Small displacements reflect merely a small prefactor in the scaling form eq.(5), and is analogous to a small diffusion constant

(which slows the diffusive process, but does not affect the scaling properties even at small spatial scales). Moreover, the asymptotic region of interest is at small u and at small $u=L$, the scaling behaviors that we focus are in small u interval. It would be possible to increase the system size and extend the scaling region of the scaling variable, $u=L$, for about two more decades.

We check the scaling form eq.(5) by collapsing the data (see Fig.(2)) with $z_s = 1.5$ in 1+1D and $z_s = 1.6$ in 2+1D. The prediction, $\beta = 1$, gives excellent data collapse, except for the non universal part around $u < 10$ in 1+1D and $u < 4$ in 2+1D. This non universal behavior is likely caused by the discrete lattice spacing. More detail of the dynamical exponent z_w must avoid this small u region while keeping $u=L$ small. In Fig.(3b) (4b), we fit z_w by omitting the data from $u < 10$ in 1+1D and $u < 4$ in 2+1D. It might appear that by ignoring data from these regions, a large fraction of information in the data is lost. In fact, only less than a quarter of the data points falls in these regions. The crossover from uncorrelated random walker behavior ($z = 2$, large $u=L$) to correlated behavior ($z \neq 2$, small $u=L$) is visible in Fig.(3b) (4b), where the exponent decreasing from 2 to z_s as the system size is increased. We conclude that $z_w = 1.50(1)$ in the 1+1D and $z_w = 1.60(1)$ in the 2+1D KK model.

Our measurement of z_w provides one of the very few independent and direct measurements of the dynamical exponent z_s on stationary state KPZ-type surfaces. Conventional approaches determine the dynamical exponent indirectly through the measurement of the scaling behaviors of the width of surfaces in the transient state while growing from a flat initial condition. The surface width defined as $W = h(h-h)^2 i^{1-2}$ scales as $W \sim t^{\beta}$ for $t \sim L^{z_s}$. Then the dynamical exponent is found by using the scaling relation $z_s = \beta/\nu$. The other possibility is to measure the correlation function $g(x;t) = h(h(x_0 + x;t_0 + t) - h(x_0;t_0))^2 i^{-\beta} (t)^2$ for $t < (x)^{z_s}$ at stationary state. Both methods obtain the dynamical exponent indirectly through the exponent β . By tracing the path of the PRW, we are able to provide an independent and direct measurement of the dynamical exponent without knowledge about the global width of the surface, with only information about the local slopes around the PRW.

Compared to the conventional methods of measuring the dynamical exponent, we only need to acquire information of the local slopes around the PRW. Thus, it is instructive to understand the connection between the slope-slope correlations along the path of the PRW

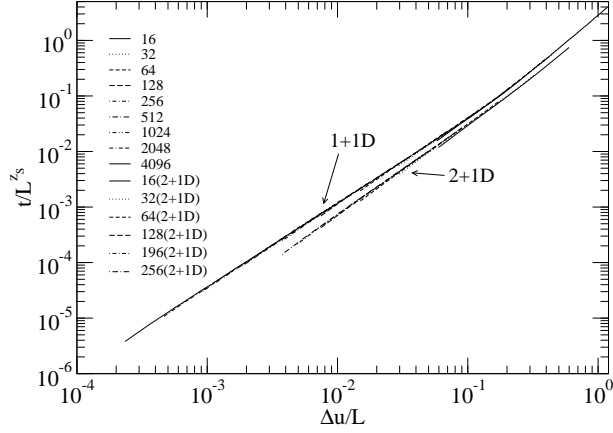


FIG .2: Collapses of t versus u . We use $z_s = 1.5$ for 1+1D, $z_s = 1.6$ for 2+1D and $\nu = 1$ for both cases.

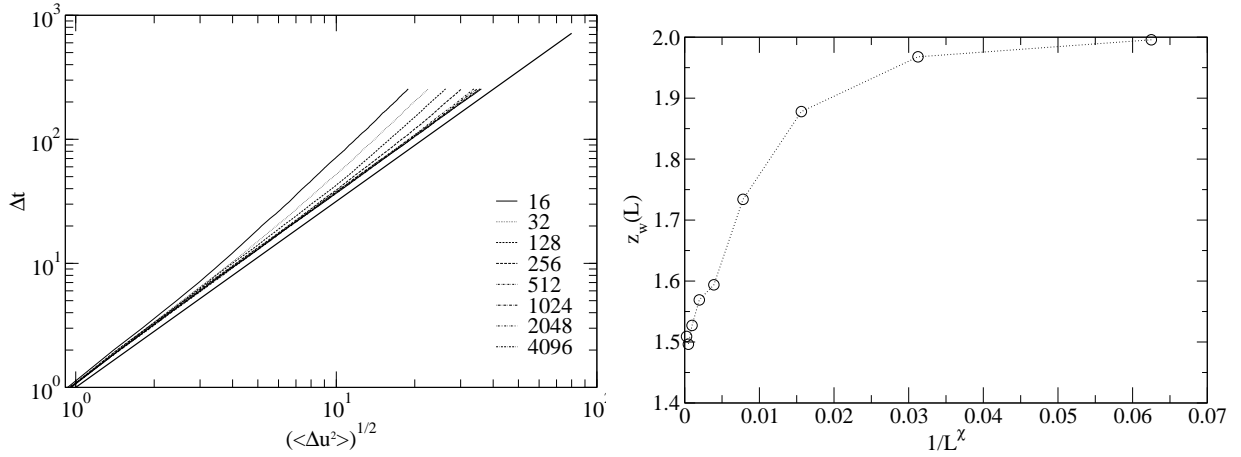


FIG .3: (a) The log-log plot of t versus u in the 1+1D KPZ model. For reference, we plot the solid line with a slope of 1.5. (b) Fitting of z_w for different system sizes in the 1+1D. It shows the crossover from free uncorrelated random walker behavior ($z = 2$) to a KPZ-type PRW behavior ($z = 1.5$). The dotted line is for the convenience to guide by eyes.

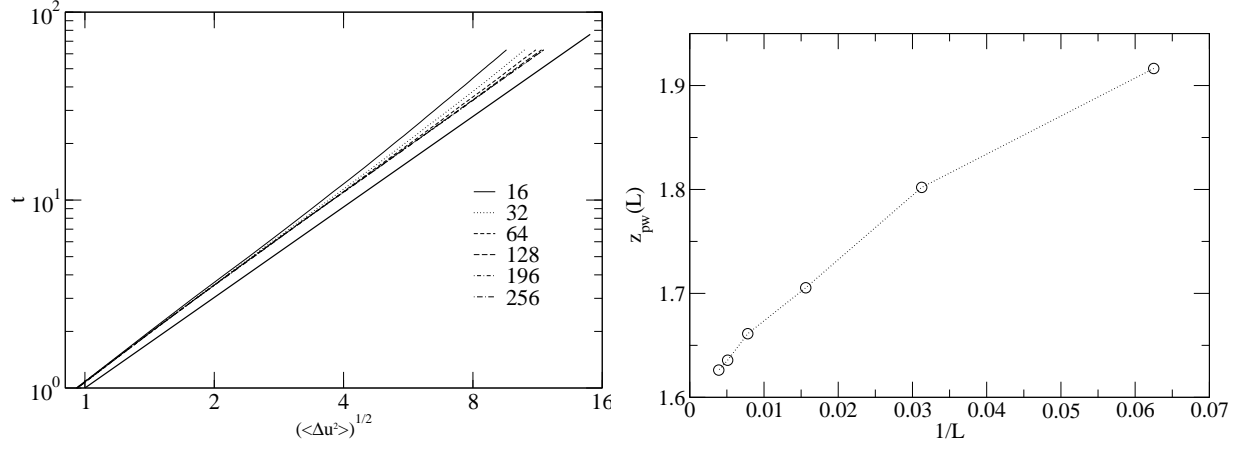


FIG . 4: (a)The log-log plot of t versus $\langle \Delta u^2 \rangle^{1/2}$ in the 2+1D KPZ model. For reference, we plot the solid line with a slope of 1.6. (b)Fitting of z_w for different system sizes in the 1+1D. It shows the crossover from free uncorrelated random walker behavior ($z = 2$) to a KPZ-type PRW behavior ($z = 1.6$). The dotted line is for the convenience to guide by eyes.

and the global roughen dynamics of the surface.

The displacement of the PRW and the correlation of the slopes are connected by the fluctuation-dissipation theory. The scaling of the dispersion in the PRW displacement can be evaluated from the slope-slope correlation function along the world line of the PRW [11], i.e.,

$$h(u(t) - u(0))^2 \sim \int_0^t dt \int_0^t dt' \langle \dot{u}(t) \dot{u}(t') \rangle \sim t^{1-z_w}; \quad (6)$$

with $\langle \dot{u}(t) \dot{u}(t') \rangle$,

$$\langle \dot{u}(t) \dot{u}(t') \rangle = \frac{\partial u(t)}{\partial t} \frac{\partial u(t')}{\partial t} + \frac{\partial}{\partial x} h(u(t); x) \frac{\partial}{\partial x} h(u(t'); x); \quad (7)$$

This correlation function $\langle \dot{u}(t) \dot{u}(t') \rangle$ is different from the conventional slope-slope correlations, $\tilde{c}(r;t) = \langle \partial_x h(r;t) \partial_x h(0;0) \rangle$, where the correlations are calculated at specified r . Instead, we need to evaluate the correlation $\tilde{c}(r;t)$ along the correlated path, the world line of the PRW, $r = u(t)$.

The most general scaling form for $\tilde{c}(r;t)$ is,

$$\tilde{c}(r;t) = b^2 \tilde{c}(b^{-1}r; b^{-z_s}t); \quad (8)$$

where \tilde{c} is an exponent yet to be determined. This scaling form is equivalent to

$$\tilde{c}(r;t) = t^{2-z_s} F(r t^{-z_s}); \quad (9)$$

with $F(y)$ a scaling function. Since the paths of the PRW are actually determined by the surface fluctuations, averaging over different paths can be approximated by averaging over different realizations of the surface (like different Monte Carlo runs). $\langle \dot{u}(t) \dot{u}(t') \rangle$ is approximately equal to the value of $\tilde{c}(r;t)$ at $r = u(t) - u(t')$. Thus, $\langle \dot{u}(t) \dot{u}(t') \rangle$ scales as

$$\langle \dot{u}(t) \dot{u}(t') \rangle \sim (t - t')^{2-z_s} F((t - t')^{-z_s}); \quad (10)$$

If $z_s > 1$, asymptotically, the scaling function behaves as $F(y^{-1}) \sim F(0) + F'(0) y^{-1}$, which approaches a constant, for $y \gg 1$. Hence the correlation function scales as $\langle \dot{u}(t) \dot{u}(t') \rangle \sim (t - t')^{2-z_s}$. With Eq. (6), we obtain $2 + 2 - z_s = 2 - z_w$. This relation allows us to determine z_w , which is the scaling dimension of the slope operator, from the measurement of z_w . Furthermore, if $z_s = 1$, then $z_w = 1$ provided that the KPZ scaling relation $z_s + z_w = 2$ holds. This result, $z_w = 1$, is consistent with Lassig's operator production expansion

scheme [4] and our previous work [6] for KPZ type surface. Namely, all slope{slope correlations can be obtained by the naive power counting and the slope operator, $\frac{\partial h}{\partial x}$, scales as x^{-1} .

Our numerical results suggest that β is indeed equal to one for upwards moving PRW s. In 1+1D, renormalization group (RG) calculations gave $\tilde{\nu}(r;t) \sim t^{1-z_s} F(r^2/t)$ [12], so our results imply the value of z is fixed as $z_w = z_s = 3/2$ for 1+1D. In 2+1D KPZ-type surface growth, RG calculations indicated that the fixed point is at strong coupling such that analytical results can not be obtained perturbatively [1]. To author's knowledge, no analytic results for the scaling form of $\tilde{\nu}(r;t)$ has been obtained for 2+1D. Our numerical results support $\beta = 1$ for KPZ-type surface.

IV. COALESCENCE OF PASSIVE RANDOM WALKERS

Why does an upwards moving PRW typically ends up on the global maximum? To further understand the mechanism of this phenomena, we study the dynamics of multiple PRW s on the KPZ type surfaces. If all upward moving PRW eventually reach the global maximum of the finite sized KPZ-type surface, then all of them will converge to the same hill top even though they start at different positions. This is true only if the PRW s have the property of coalescence, namely, two PRW s close to each other merge into each other and move together afterward during the process of moving up to the global maximum.

Although, in the definition of the dynamics of the PRW s, the PRW s always moves upward, this simple coupling between the PRW and the surface only guarantees that the PRW reaches a local maximum, not the global one. Suppose that the PRW s remain trapped on local hill tops. Different PRW s will have their own independent world lines in space-time. We find that in KPZ dynamics with negative β the upwards moving PRW coalesce. Two PRW s separated over a distance r at time $t = 0$ merge into each other after a typical time period $t \sim r^{z_w}$ as shown in Fig.(1) (see also (8a)). On the contrary, downwards moving PRW s do not coalesce in $\beta < 0$ KPZ-type dynamics and PRW s do not coalesce in Edward-Wilkinson (EW) type growth (the $\beta = 0$ point of KPZ equation).

Consider that the PRW s sitting on two nearby hill tops which have similar heights. The region between the two hill tops is a small and shallow valley. If both the hill tops and the valley is relatively higher than the other parts of the surface, the valley is likely to be filled

up and vanish in a short time. These two hill tops merge and the merging event causes the PRW s to coalesce afterward as shown in Fig.(1). The coalescence of the PRW s is equivalent to the merging of two nearby hill tops.

This trivial argument seems to imply that PRW s will coalesce for any type of growing surface as long as the PRW s are trapped on hill tops. This is not true. We found that the PRW s on EW type surface do not coalesce, although the KPZ type surface and the EW -type surface have the same stationary state and roughness exponent $\alpha = 1/2$ in $1+1$ D. The following discussion and the detail analysis in Sec.V show how the nonlinear term, $(\partial_x h)^2$, in the KPZ equation (eq.(1)) affect and create the phenomenon of coalescence.

The nonlinear term, $(\partial_x h)^2$, in the KPZ equation controls how the growth rate depends on local slopes. Consider a plateau on a surface, for positive ν , the growth rate on the slope parts of the plateau is larger than the ν at top hence the ν at top of the plateau expands by lateral growth on the slopes and the hill tops become flatter than the valleys. Negative ν has an opposite effect, the slope parts grows slower than the ν at tops hence the ν at tops become sharper. Shrinking of plateau ν at tops is an indication for a negative ν in the KPZ equation. The merging events of two hill tops is equivalent to shrinking of ν at top plateaus. For example, at larger length scales, the shallow valley between two nearby hill tops and the hill tops themselves as a whole acts like a plateau on the surface (Fig.(5)). Before the coalescence of the hill tops, the size of the ν at top of the plateau is the distance between these two hill tops. While these two hill tops are moving towards each other by surface fluctuations, the size of the ν at plateau top effectively shrinks, which is an indication of a negative ν . In the KK model, ν is negative and the origin of negative ν is due to the restricted solid-on-solid condition $|h_{ij} - h_j| \leq 1$, which reduces the growth rate to zero at the regions where the density of $h = 1$ (or $h = -1$) steps is one. With negative ν for KK model, which belongs to KPZ universality class, both the hill tops and the PRW s coalesce.

V. COALESCENCE OF HILL TOPS IN NOISELESS KPZ EQUATION

We can gain insights about the coalescence of the PRW s on KPZ type surface by investigating the solution for noiseless KPZ equation in the limit $\eta \rightarrow 0$. In that limit, the evolution of surfaces with given initial conditions has analytical solutions, which allow us to study the details of the dynamics of the hill tops.

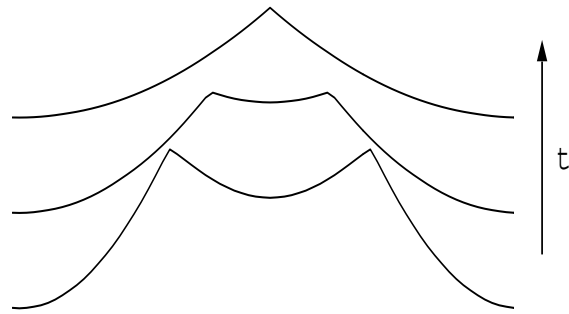


FIG .5: A close look of the coalescence of two hill tops driven by the noiseless KPZ equation. The curves in this figure have been shifted for clarity. The two hill tops have a common contact point at the bottom of the valley between them .

A detailed derivation of the solution for noiseless KPZ equation can be found in [13]. We only present a brief review of the derivation. With the Hopf-Cole transformation, $(x;t) = \exp(-h(x;t))$, we can transform the noiseless KPZ equation into a simple linear diffusion equation for $(x;t)$,

$$\frac{\partial}{\partial t} = \frac{\partial^2}{\partial x^2}; \quad (11)$$

The solution is a superposition of Gaussian functions weighted by the initial conditions,

$$(x;t) = \int dy (y;0) \exp\left(-\frac{(x-y)^2}{t}\right); \quad (12)$$

where $(y;0) = \exp(-h(y;0))$ is the initial condition, determined by the initial height profile $h(y;0)$. In the limit $t \rightarrow 0$, we can simplify the solution by introducing the velocity, $v = \partial_x h$, as an auxiliary variable,

$$v = -\frac{\partial \ln}{\partial x} = \frac{\int dy \frac{2(x-y)}{t} \exp\left(-\frac{(x-y)^2}{t} + h(y;0)\right)}{\int dy \exp\left(-\frac{(x-y)^2}{t} + h(y;0)\right)}; \quad (13)$$

By the method of steepest descent in the limit $t \rightarrow 0$, this yields

$$v(x;t) = \frac{2(x - y_{\text{in}}(x;t))}{t}; \quad (14)$$

where y_{in} is a function of both x and t , and it is determined by taking y at where $\frac{(x-y)^2}{t} + h(y;0)$ is minimum for fixed values of x and t . Namely,

$$y_{\text{in}}(x;t) = \arg \min_y \left[\frac{(x-y)^2}{t} + h(y;0) \right]; \quad (15)$$

The $y_{\text{in}}(x;t)$ are usually only piecewise continuous functions of x , particularly for random initial conditions generated by random walkers. Shock waves of the velocity field are formed at where $y_{\text{in}}(x;t)$ is discontinuous.

Assuming $y_{\text{in}}(x;t)$ is constant between x and y_{in} , we can further integrate $v(x;t)$:

$$h(x;t) = \frac{(x - y_{\text{in}}(x;t))^2}{t} + c_h; \quad (16)$$

where c_h is the integration constant. The solution for $h(x;t)$ is reduced to the problem of finding y_{in} and c_h .

Determining y_{in} for $t < 0$ is equivalent to finding the y for which that the vertical distance is the shortest between the initial height configuration, $h(y;0)$, and the parabola, $\frac{(x-y)^2}{t}$, centered at x , while the parabola is approaching the surface from below. y_{in} is the

first contact point between the two curves $h(y;0)$ and $(y;x;t) = \frac{(x-y)^2}{t} + c$ while c is adjusted to $c(x;t) = h(y_{m_{in}};0) - \frac{(x-y_{m_{in}})^2}{t}$ (Fig.(6)). The contact point $y_{m_{in}}$ is where $h(y;0) - \frac{(x-y)^2}{t}$ is a minimum. Once $y_{m_{in}}$ is found, $h(x;t)$ follows from eq.(16) with $c_h = h(y_{m_{in}};t)$. Thus, we have $h(x;t) = (x;x;t) = c(x;t)$, which is the top of the parabola. The surface between x and $y_{m_{in}}(x;t)$ is parabolic in shape at time t . It is possible that there exists more than one first contact point for certain x and t . If this happens, $y_{m_{in}}(x;t)$ as a function of x will be discontinuous at that specific x .

This solution has an intuitive graphical interpretation, which is useful for understanding the coalescence phenomena. The evolution of the surfaces is generated by a sequence of geometry transformations on the surfaces at a earlier time. For negative τ , the new surface at time t is obtained by scanning the original surface from below with a probe that has a parabolic shaped tip, $(y;x;t) = \frac{(x-y)^2}{t} + c(x;t)$ (Fig.(6)) for negative τ . (For positive τ , the probe scans the surface from above instead.) The probe is centered at position x , and $c(x;t)$ (the vertical position of the top of the tip) is adjusted by moving the probe up and down. When the probe approaches the surface from below, it stops when it starts to come into contact with the surface. The horizontal position of the first contact point between the probe and the surface is $y_{m_{in}}(x;t)$. Since the probe stops to move upward once it comes in contact with the surface, we might think the vertical position of the tip of the probe, $c(x;t)$, as the height of the new surface seen by the probe at x at time t . The probe scans through the surface and plots a new surface that gives the surface evolved by the noiseless KPZ equation at a later time. Because the parabolic shape of the probe, the new surface usually consists of a collection of parabola shaped segments (the dashed curves shown in Fig.(6)).

With this geometrical interpretation of the exact solution of the noiseless KPZ equation, we are able to visualize how the singular hill tops are formed and to discuss the dynamics of coalescence of the hill tops. If the local average curvature over a region such as between A and C in Fig.(6) is larger than the curvature of the tip of the probe at time t , then the tip can not reach the surface everywhere between point A and C. When the probe scans through this region, at point B in Fig.(6), there are two first contact points for the parabola, and $y_{m_{in}}(x)$ is discontinued at this point. At points where the function $y_{m_{in}}(x)$ is not continuous, the path of the tip forms a cusp, which is a hill top of the new surface. The position of the hill top is determined by the positions of the two contact points A, C and the curvature of

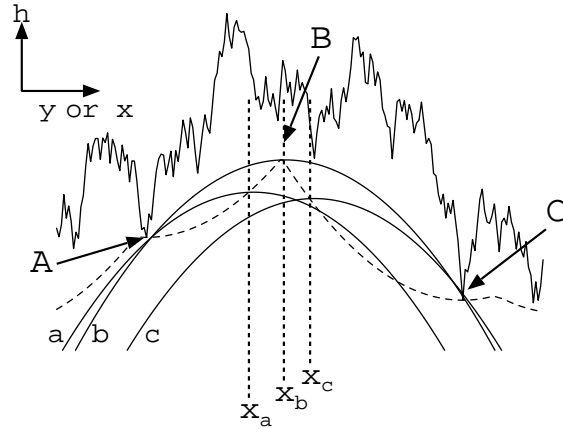


FIG . 6: The parabolic shape probe tip scans through point x_a , x_b , and x_c from left to right. Curve (a), (b), and (c) are parabola which are centered at x_a , x_b , and x_c respectively. Curve (a) / (b) only contact with the initial random surface at point A / B. Curve (b) contacts with the initial surface at both point A and C. While the probe is scanning through x_b , the first contact point jumps from A to C. Thus, $y_{min}(x)$ is discontinued at point x_b and the path of the tip create a cusp at point C. The dashed curve is the surface generate by the path of the probe tip.

the probe tip.

We can also write the solution of $h(x;t)$ as a functional transformation T defined as

$$T_t(h(x;t_0)) = h(x;t + \frac{1}{2} \sqrt{4t(x - y_0)^2 + h(y_0;t_0)^2}) \quad (17)$$

This transformation has the following property,

$$T_{t_1+t_2}(h(x;t_0)) = T_{t_2} T_{t_1}(h(x;t_0)) \quad (18)$$

The geometrical interpretation of the solution in this form is similar to the Huygens principle growth algorithm [14], except that parabola shaped wave fronts instead of circular or spherical wave fronts are used. The transformation eq.(17) can be applied iteratively and is suitable for evaluating the evolution of the surface numerically.

We evaluate the evolution of a random initial surface with Eq.(17). The coalescence of the hill tops is shown clearly in Fig.(7a). Why do those hill tops coalesce and how do they move? Will hill top B in Fig.(6) move towards point A or point C? Answers to these questions can be addressed from the equation of motion of the hill tops.

The curvature of the probe at time t is equal to $1/(2t)$. The probe becomes broader and broader with time. As long as the absolute value of the local curvature around the contact points, A or C, is much larger than the absolute value of the curvature of the probe, the positions of these two contact points do not change. In that case, the height difference $h(x_A;t) - h(x_B;t)$, where x_A and x_C are the horizontal coordinates of points A and C respectively, is also constant. Furthermore,

$$h(x_A;t) - h(x_B;t) = (h(x_A;t) - h(x_C;t)) - (h(x_C;t) - h(x_B;t))$$

The curve between A and B and the curve between B and C of the new surface are two parabolas. With $h(x_A;t) - h(x_B;t) = (x_A - x_B)^2/(2t)$ and $h(x_C;t) - h(x_B;t) = (x_C - x_B)^2/(2t)$, we obtain the equation of motion of the hill top,

$$\frac{\partial x_B}{\partial t} = -\frac{1}{2} \frac{x_A + x_C}{x_B} \quad (19)$$

This equation implies that the hill top always moves toward the closest of the two contact points. Moreover, the closest contact point is also the higher one. If two neighboring hill tops share the same contact point, and that contact point is the highest one for both hill

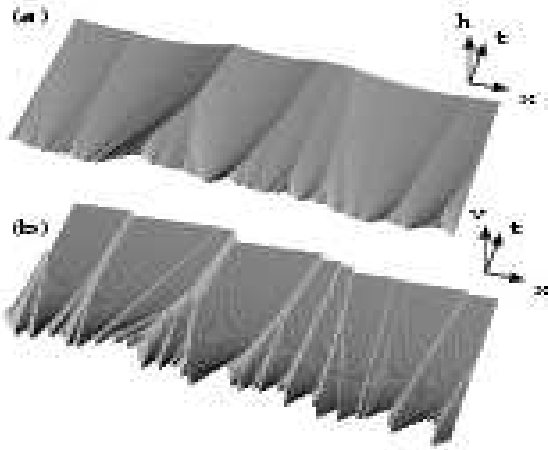


FIG . 7: (a) The evolution of the surface under transformation eq.(17). Hill tops coalesce and form tree-like structure. (b) The coalescence of shock waves in the velocity field. The velocity is defined as $v = \frac{\partial h}{\partial x}$.

tops, then these two hill tops will merge into one around the position of the shared contact point as illustrated in Fig.(5). A sequence of coalescence events of the hill tops forms a tree like structure world lines as in Fig (7a).

The dynamics of the coalescence of hill tops in the noiseless KPZ equation is totally deterministic and only depends on the initial surface. In the noisy case, the dynamics becomes stochastic, however, the qualitative behavior of the coalescence of the hill tops is still sustained even when the surface is perturbed with random ly depositions. The nonlinear term causes the coalescence of the hill tops and remains essential even when the dynamics is stochastic. To check that the nonlinear term is responsible for the coalescence in the stochastic dynamics, we apply our upwards moving PRW model to EW -type surfaces. The upwards moving PRW s for EW type surface don't coalesce although the density of the PRW s is higher on the hill tops.

V I. D O W N W A R D S M O V I N G P A S S I V E R A N D O M W A L K E R S

So far we focused on the case where α and β have opposite signs, i.e., when the PRW s move upward ($\alpha > 0$) in the KK model ($\beta < 0$). The discussion in the previous section suggests that the shape of the surface has a very different character between a hill top and a valley bottom on the surface with noiseless KPZ dynamics, namely, hill tops are sharp with discontinued slopes while valley bottoms are rounded and with continuous slopes. The symmetry is broken by the nonlinear term. We also found that valley bottoms vanish by themselves, instead of coalescing with others valleys.

If α is negative, the PRW s move toward the valley bottoms. It is interesting to see how the PRW s respond to such qualitative aspects of the surface in the presence of stochastic noise. In the deterministic case, the hill tops and valley bottoms intertwine with each other, the number of valley bottoms and the number of hill tops both decrease. This is not true for the stochastic case. New microscopic hill tops and valley bottoms are being formed constantly by the noisy depositions of particles. Is the coalescence of the PRW s stable under such perturbations? For upwards moving PRW s in the KK model, coalescences are stable against the noise. As we will see next, the coalescence of the downwards moving PRW s is not stable against random depositions.

Consider the upwards moving PRW s. Suppose noise splits the hill tops by creating a

small valley between them. This small valley is unstable against the dynamics as we have seen in the previous section. These two hill tops will merge again soon as a result due to the nonlinear term in KPZ equation. The nonlinear KPZ dynamics stabilizes the coalescence of the upwards moving PRW s.

Next, imagine several downward moving PRW s moving into the same valley. The aggregation of the PRW s is not stable against the perturbation. Depositions of particles on the valley split the valley. A PRW on the original valley bottom can go to either one of those two valleys with equal probability, so both valleys will be occupied by PRW s. Do the new created subvalleys always merge back into each others? A valley bottom does not move in the noiseless case, they will remain separated by the hill top. The hill top does not vanish unless it is driven away to merge with other hill tops which is a much less likely process than the splitting. Therefore, dynamics like this does not stabilize the aggregation of downwards moving PRW s. They tend to be separated under the growth dynamics and we expect that the dynamics of downwards moving PRW s, trapped in a valley bottom s, is dominated by the perturbation of random deposition rather than the deterministic nonlinear term in the dynamics. In Fig.(8c), we show a typical simulation for downwards moving PRW s. Instead of coalescence, we find that the aggregation clusters of PRW s are not stable and split constantly.

Coalescence of the upwards moving PRW s for negative β is an important feature of KPZ-type surfaces. Not only does it ensure that the PRW s end-up trapped on the global maximum. It also reveal the space-time structure of KPZ-type surfaces in detail, i.e., hill tops (valley bottom s) coalescence as time evolving for negative (positive) β .

Our analysis on KPZ equation applies to the phenomena of coalescence of the shock waves in the inviscid ($\nu = 0$) noiseless Burgers equation. The velocity in the Burgers equation is the slope of the surface in KPZ-type surface, i.e., $v = \partial_x h$. By differentiation of eq. (1), it becomes

$$\frac{\partial v}{\partial t} = -v \frac{\partial v}{\partial x} + \frac{\partial^2 v}{\partial x^2} + \eta_B \quad (20)$$

The noise term satisfies $\langle \eta_B(x;t) \eta_B(0;0) \rangle = \delta_x^2(x) \delta(t)$. Because the slopes of the surface are discontinuous at the hill tops, the hill tops on KPZ-type surface correspond to the shock waves in the Burgers equation. The coalescence of the hill tops of the surface indicates that the shock waves coalesce, as illustrated in Fig.(7(b)). Coalescences of shock waves described by noiseless Burgers equation have been reported in a numerical study of inelastic collisions

of particles in 1+1 dimensions[15]. Bohr and Pivovskiy also showed that the zeros in the velocity field of Burgers equation coalesce[11]. The above analysis for the coalescence of KPZ hill tops translates directly into the coalescence of shock waves in the Burgers equation with noise. Our analysis on coalescences of PRW s on a growing surface presented here not only provides further intuitive and detailed understanding the mechanism of these coalescence phenomena but also explains, in both deterministic and stochastic dynamics, the different behaviors between hill tops and valleys, which are distinct types of zeros in the velocity field in the Burgers turbulences.

VII. RIVER-LIKE NETWORK AND PASSIVE SCALARS

To further understand the stability of the aggregations of PRW s, we study how random forces, in addition to the driving force from the surface slope, are applied to the PRW s directly, change the tree-like structure of the PRW world lines in Fig.(8a). Is the tree-like structure stable? Random noise modifies the equation of motion of the PRW as

$$\frac{\partial u}{\partial t} = \frac{\partial}{\partial x} h(x;t) \dot{x} = u(t) + \eta_w(x;t); \quad (21)$$

with η_w the uncorrelated noise, $\langle \eta_w(x;t) \eta_w(0;0) \rangle = D_w \delta(x) \delta(t)$. D_w is the diffusion constant of the PRW if $\eta = 0$.

First consider a single PRW on a surface. The second term on the right hand side of eq.(21) introduces the ordinary diffusive behavior, i.e., $u(t) \sim (D_w t)^{1/2}$. The scaling behavior due to the deterministic first term, $u(t) \sim (K_w t)^{1/z_w}$, (K_w is a constant determined by η and η) still dominates the large scale behavior since $1/z_w > 2$. However, the PRW appears as diffusive instead of super-diffusive at length scales smaller than $l_c = \frac{D_w}{K_w} \frac{1}{2 - z_w}$.

The diffusive noise also affects the coalescence of multiple PRW s. For small perturbations, the aggregation is stable because the PRW s can not escape from the hill top by diffusion if the hill top is high and large enough. The net effect of diffusions simply broadens the coalescence clusters. However, if we increase the strength of the random noise, the PRW s can escape from the hill top and be caught by other hill tops nearby with finite probability. In this case, a cluster of coalescence PRW s splits and the world lines of the PRW s form a braid-like network instead of a tree structure. A typical configuration of such a braid-like network is shown in Fig.(8b). Both the tree-like and the braid-like network resemble

river-like networks of different length scales in Nature [16].

The crossover scale between tree-like network and braid-like network is given by l_c . We observe diffusive behaviors locally both at a scale less than l_c near a cluster. The braid-like network emerges at the crossover scale, l_c , and the tree-like structure is recovered in a scale much larger than l_c .

Furthermore, we can consider the evolution of the probability distribution function $P(\mathbf{x};t)$ of finding a particle at position \mathbf{x} at time t . Note that the total number of PRWs is conserved in our model. Therefore, $P(\mathbf{x};t)$ has the standard conserved form,

$$\frac{\partial P(\mathbf{x};t)}{\partial t} = -\nabla \cdot \mathbf{j}(\mathbf{x};t); \quad (22)$$

where $\mathbf{j}(\mathbf{x};t)$ is the PRW current. The current is the sum of the advected part and the diffusive contribution, i.e., $\mathbf{j}(\mathbf{x};t) = vP(\mathbf{x};t) + D_w \nabla_x P(\mathbf{x};t)$. Hence, we have

$$\frac{\partial P(\mathbf{x};t)}{\partial t} = -\nabla \cdot (vP(\mathbf{x};t) + D_w \nabla_x P(\mathbf{x};t)); \quad (23)$$

This is simply the equation of motion of a passive scalar $P(\mathbf{x};t)$ in a fluid. In the limit $D_w \rightarrow 0$, the passive scalar will be concentrated at a globe hill top as we have seen in the previous sections if v and κ has opposite sign for a finite system.

VIII. CONCLUDING REMARKS

Motivated by the domain wall dynamics on nonequilibrium fluctuating surfaces, we study the dynamics of passive random walkers on a KPZ-type growing surface. We show that, although the coupling rule between a PRW and a surface is defined locally, a PRW typically reaches the maximum of the surface over a distance x in a time scale $t \sim x^z$ and "feels" the fluctuations of the surface over the same length scale. Two PRWs separated by x coalesce after $t \sim x^z$. The fluctuations of the position of such a PRW follow the same dynamical scaling as the KPZ fluctuations. We verify this scaling behavior numerically. Tracing the path of the PRWs on KPZ-type surface is an effective method to measure the dynamical exponent directly in the stationary state.

In addition to the scaling, the dynamics of passive random walkers reveals detailed specific space-time structures of a KPZ-type growing surface, i.e., hill tops coalesce with each other and the world lines of the PRWs form self-affine tree-like structures. We provide an analytical

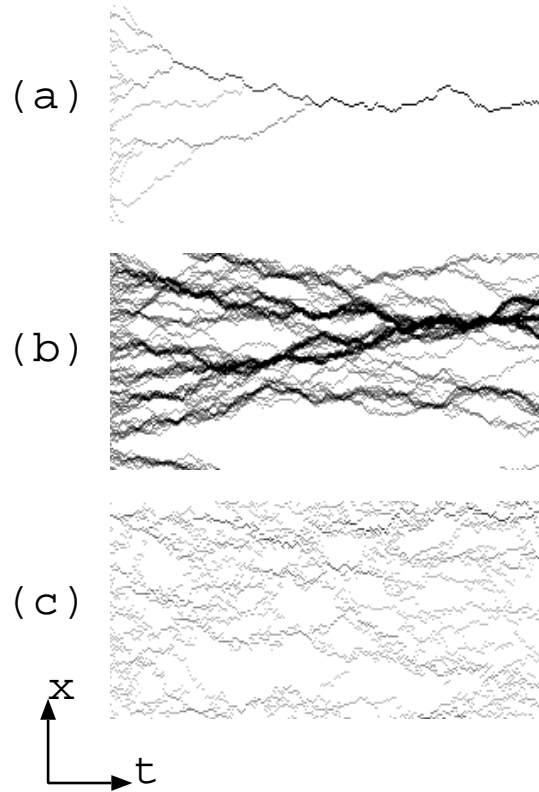


FIG. 8: World lines of passive walkers for different parameters. The lines are the path of 128 PRW on a system of size $L=128$. The darkness is proportional to the number of PRW for each site. In (a), the system is simulated in the limit $l_c = \frac{D_{PW}}{K} \frac{1}{z} \neq 0$ for upward moving PRW. In (b), we choose $l_c = L$, the system size. (c) is the result of downwards moving PRW in the limit $l_c \neq 0$. Even without a diffusion term in eq. (21), the downwards moving PRW do not coalesce. The dynamics of the downwards moving PRW on KK-type surface is dominated by the uncorrelated random depositions.

argument explaining this phenomena based on the noiseless Burgers-KPZ equation. We show how the nonlinear term $(\partial_x h)^2$ is responsible to this nontrivial coalescence phenomena in both the noiseless and noisy case. The noiseless KPZ equation also allow us understand why downwards moving PRW s do not coalesce, due to the asymmetry between hill tops and the valley bottoms.

We want to emphasize that the effectively attractive interaction which makes the PRW s coalesce is not only topological but also robust against perturbations. For KPZ-type growth, the $(\partial_x h)^2$ term breaks the symmetry between hill tops and valley bottoms during growth and introduces nontrivial dynamics of the hill tops for negative ν , and valley bottoms positive ν . The singularities on the surface generated by the nonlinear terms stabilize the aggregations of the PRW s against other perturbations. The coalescence of PRW s reveals one of the important features of the complicated space-time structure of the surface. An interesting extension of this study is to see how this generalizes to different universality classes of surface dynamics. We already point out that in EW growth, because of the particle-hole symmetry, PRW s do not coalesce. For other nonlinear models, in which the nonlinear terms break up-down symmetry, PRW s may be driven in other nontrivial ways and the surface may show interesting space-time structures.

Depending on the strength of the noise applied to the PRW s, the world lines of PRW s form tree-like or braid-like networks in space-time. The tree-like or the braid-like networks resemble river type networks in nature. The braid-like networks are the result of two competing mechanism, namely, the coalescence between PRW s caused by the fluctuations of the surface and the diffusion of PRW s caused by directly applied noise. These two mechanisms define a crossover length scale l_c , and give rise to the braid-like network. One might expect to see similar crossover phenomena in the study of passive scalars in Burgers turbulence.

Previous studies on fluctuating nonequilibrium surface were focused on the scaling behavior. This study shows that, beyond global scaling laws, like the scaling of the global interface width, nonlinear surface growth dynamics leads to intriguing detailed aspects of their space-time structures. We hope studying these different perspectives of nonequilibrium dynamics can lead to better understanding about these complex systems.

This research is supported by the National Science Foundation under grant No. DMR-9985806. The author thanks Marcel den Nijs for many useful discussions and critical reading

of the manuscript.

- [1] M .K ardar, G .P arisi, and Y .C .Zhang, *Phys.Rev.Lett.* 56, 889 (1986).
- [2] J.M .K in and J.M .K osterlitz, *Phys.Rev.Lett.* 62, 2289 (89).
- [3] T .H alpin-H ealy and Y .C .Zhang, *Physics Reports* 254, 215 (1995).
- [4] M .L assig, *Phys.Rev.Lett.* 80, 2366 (1998).
- [5] M .K otrlá, F .S lanina, and M .P redota, *Phys.Rev.B* 58, 10003 (1998).
- [6] C .S .C hin and den N ijs, *Phys.Rev.E* 59, 2633 (1999).
- [7] M .K otrlá and M .P redota, *Europhys.Lett.* 39, 251 (1997).
- [8] B .D rossel and M .K ardar, *Phys.Rev.Lett.* 85, 614 (2000).
- [9] C .S .C hin and den N ijs, *Phys.Rev.E* 64, 031606 (2001).
- [10] M .den N ijs, *J.Phys.A* 18, L549 (1985).
- [11] T .B ohr and A .P ikovsky, *Phys.Rev.Lett.* 70, 2892 (1993).
- [12] D .F orster, D .R .N elson, and M .J .S tephen, *Phys.Rev.A* 16, 732 (1977).
- [13] W .A .W oyczynski, *Burgers-KPZ Turbulence* (Springer, 1998).
- [14] C .T ang, S .A lexander, and R .B ruin sm a, *Phys.Rev.L* 64, 772 (1990).
- [15] E .B en-N ain , S .Y .C hen, G .D .D oolen, and S .R edner, *Phys.Rev.Lett.* 83, 4069 (1999).
- [16] I.R odriguez-Iturbe and A .R inaldo, *Fractal River Basins* (C am bridge U niversity P ress, 2001).